Cross-Polarization Interference Compensation for Dual-Polarization Satellite Receivers

Svilen Dimitrov *German Aerospace Center (DLR), Satellite Networks Department, 82234 Wessling, Germany, e-mail: svilen.dimitrov@dlr.de*

***Abstract*—In this paper, simultaneous transmission on two orthogonal antenna polarizations in a polarization division multiplexing (PDM) fashion is studied for wideband satellite communication links using dual-polarization satellite receivers for the purpose of doubling the data rate. In order to mitigate the cross-polarization interference (XPI), a new digital blind and transparent XPI compensation method is presented, XPI correlation learning estimation and adaptive reduction (XPI-CLEAR). The received carrier-to-interference ratio C/I and carrier-to-noise-and-interference ratio $C/(N+I)$ performance with this non-data-aided and non-decision-directed method is assessed in the XPI channel with effects such as imperfect cross-polarization discrimination (XPD) of the antennas at the transmitter and the receiver, depolarization due to atmospheric conditions, and differential frequency offset (DFO) between the two channels. The application of the XPI-CLEAR method presents considerable energy efficiency improvements for all the studied XPI channel effects, and is particularly beneficial for higher-order modulation. As a result, the XPI-CLEAR method is a practical solution to increase the data rates of the satellite air interface and to achieve the doubling of the throughput of the satellite link by the use of PDM.**

***Index Terms*—Satellite communications, polarization division multiplexing (PDM), cross-polarization interference (XPI), XPI-CLEAR, dual-polarization receiver, higher-order modulation, energy efficiency.**

I. Introduction

Satellite communications are an important component of today's information society. Beside the customary application areas, e.g., digital satellite television, Earth observation, and professional satellite networks, additional use cases have emerged, such as the global internet access via satellite and backhauling of 5G/6G base stations via satellite as part of non-terrestrial networks (NTN). Recently, an increasing number of satellites have been deployed to provide internet connectivity in remote areas, ships, airplanes and trains, e.g., Ka-Sat 9A of Eutelsat, ViaSat-1, ViaSat-2, ViaSat-3 and Starlink of SpaceX. Nowadays, satellite communications are recognized as a integral part of the 5G/6G communications architecture with the important role of providing global network coverage. For this purpose, in addition to geostationary-Earth-orbit (GEO) high-throughput satellite (HTS) systems, low-Earth-orbit (LEO) satellites are becoming increasingly popular, due to the inherent shorter transmission delays and better suitability to low-latency applications.

A number of satellite applications require high data rates over large bandwidths, e.g., satellite downlinks for Earth observation, gateway feeder links for direct-to-home internet and backhauling satellite links for mobile base stations. Due to the limitation of the available radio frequency (RF) spectrum, polarization division multiplexing (PDM), i.e., simultaneous transmission on two orthogonal antenna polarizations, using the same carrier frequency, has the potential to double the data rate of such high-bandwidth communication links. While current multi-beam satellite systems utilize a 4-color reuse scheme with two frequency bands and two polarizations for the user links [1], future multi-beam satellite systems can benefit from PDM to increase the system capacity by using both polarizations in the same beam. Depending on the communication scenario, the PDM setup can be realized either by using dual-polarization antennas at the satellite and the gateway or user terminal, or by using two co-located satellites with single-polarization antennas and two single-polarization antennas at the gateway or user terminal. An example of an operational dual-polarization satellite system utilizing PDM technology for Earth observation is WorldView-3 [2].

Because of imperfections of the antennas at the transmitter and the receiver, as well as due to the effects of the atmosphere caused by water droplets and ice crystals, the two polarizations are not completely orthogonal, resulting in cross-polarization interference (XPI). The XPI is higher with the increase of the carrier frequency, e.g. in Ku, Ka, and Q/V band, and at lower elevation angles due to a longer propagation path through the atmosphere. The increased XPI between the two channels reduces the carrier-to-interference ratio C/I and, as a result, the carrier-to-noise-and-interference ratio $C/(N+I)$ at the receiver, which degrades the performance of the demodulator and decoder. In state-of-the-art LEO-satellite systems for Earth observation [1], [3], adaptive coding and modulation (ACM) is employed to adjust the modulation format according to the elevation-dependent XPI and the resulting $C/(N+I)$ conditions during the satellite visibility window. A high XPI is, therefore, a limiting factor for the application of higher-order modulation formats and the achievable data rates. In order to mitigate the effects of this time-variable XPI, an adaptive receiver algorithm performing XPI estimation and compensation is required.

Proprietary solutions have been developed to compensate the XPI at the receiver. Based on an adaptive filter architecture with access to the signals on both polarizations prior to the symbol demapping and decoding stages, an XPI cancellation (XPIC) method has been described in [4]. It can be applied on the signals of the two polarizations either in a symbol-spaced or a fractionally-spaced fashion. The adaptive filters for the intended and interfering paths are trained to generate signals used for the XPI cancellation. The training of the filters can be decision-directed and without prior knowledge of pilot symbols, i.e. blind, only requiring knowledge of

the used modulation format at the receiver. The training can also be data-aided by means of known pilot symbols at the expense of additional signaling overhead. A closely related cross-polarization digital equalization and automatic filtering (XDEAF) method has been presented in [5]. An extension to the XPIC method for operation in scenarios with a differential frequency offset (DFO) between the two channels due to, e.g., not perfectly synchronized frequency conversion is presented in [6], including additional electronic components at the expense of higher receiver complexity. While these approaches reduce the XPI, they also increase the computational complexity of the receiver, due to the required training and XPI compensation with multiple filter coefficients, which can be a constraint for the implementation in high-rate hardware devices and applications. Space-time coding and spatial modulation have also been presented for dual-polarized mobile satellite communications [7], [8]. For their successful demodulation, however, these solutions require channel state information at the receiver (CSIR). In the presence of the time-variant XPI, the CSIR can be obtained by means of frequent data-aided channel estimation using known pilot symbols at the expense of additional signaling overhead. In addition, due to the joint pre-processing of the two signals at the transmitter, these solutions have stringent synchronization requirements on the transmitter hardware which can increase the cost of the space segment.

In this paper, a new digital XPI compensation method is presented: XPI correlation learning estimation and adaptive reduction (XPI-CLEAR) [9], [10]. The digital XPI-CLEAR method is applied in a dual-polarization satellite receiver, simultaneously processing the signal samples on both channels. This non-data-aided and non-decision-directed method uses the correlation between the two received signals for the adaptive estimation and cancellation of the XPI in a blind and transparent fashion. It can be applied in receivers with independent frequency conversion blocks for the two channels, and it can operate in the presence of DFO between the received signals. It has a lower complexity as compared to the filter-based approaches, and is therefore suitable for higher-rate applications. While the focus of this study is on the use with DVB-S2X [1] and CCSDS [3] waveforms, the XPI-CLEAR method can also be applied with future New Radio (NR) waveforms for NTN [11], as long as the signals of the two polarizations have the same bandwidth, the same carrier frequency and the same spectrum shape. The performance of a dual-polarization satellite receiver implementing the XPI-CLEAR method is simulated in terms of the received C/I and $C/(N+I)$, using an XPI channel model with effects such as imperfect cross-polarization discrimination (XPD) of the antennas at the transmitter and the receiver, depolarization due to atmospheric conditions, and DFO between the two channels. The application of the XPI-CLEAR method presents considerable improvements of the received $C/(N+I)$ over the operational range of ACM for all the studied XPI channel effects, and is particularly beneficial for higher-order modulation. As a result, the XPI-CLEAR method is a practical solution to increase the data rates of the satellite air interface and to achieve the doubling of the throughput of the satellite link by the use of PDM.

The rest of the paper is organized as follows. Section II presents the satellite system model, including the transmission chain and the channel modelling. Section III describes the XPI-CLEAR method for compensation of the XPI channel. Section IV presents the performance evaluation results. Finally, Section V concludes the paper.

II. System Model

In a dual-polarization satellite communication system for Earth observation, a satellite or a pair of collocated satellites transmit message signals over two channels in a polarization-division multiplexing (PDM) fashion to a ground station using a single antenna or a pair of antennas. For example, one channel utilizes a right-hand circular polarization (RHCP), alternatively a vertical polarization (VP), and another channel utilizing a left-hand circular polarization (LHCP), alternatively a horizontal polarization (HP). The imperfect decoupling of the cross-polarization signals at the antenna introduces cross-polarization interference (XPI) from one signal into the other. Transmission over this dual-polarization channel with XPI results in a degradation of the performance of the satellite receiver, and consequently in a reduction of the achievable data rates. In order to alleviate the issue, a dual-channel receiver can employ XPI compensation, using the locally available information of the XPI within the two received signals. In this section, the transmission chain, the dual-polarization channel model, and a proposed XPI compensation method are presented.

A. Dual-Polarization Satellite Transmission Chain

The block diagram of a dual-polarization satellite communication system with XPI is presented in Figure 1. At the dual-polarization transmitter side, a stream of data bits in each of the two channels are encoded by means of a forward error correction (FEC) scheme, and modulated for transmission. In DVB-S2X [1], first, a Bose-Chaudhuri-Hocquenghem (BCH) encoder is applied, followed by an low-density parity check (LDPC) encoder and bit interleaver. The resulting FEC frames are mapped to symbols, using amplitude and phase shift keying (APSK) modulation with constellations up to 256-APSK at the modulator. The modulated symbols are grouped in physical-layer (PL) frames, and scrambled by different scrambling sequences in the two channels, in order to ensure the decorrelation of the two signals. The two signals are then oversampled by a chosen oversampling factor and pulse shaped by means of a square root raised cosine filter (SRRCF) to ensure spectrum integrity of the waveform for radio-frequency (RF) transmission. After digital-to-analog conversion (DAC), the signals are up-converted to the carrier frequency, e.g., in the Ka band, and amplified for transmission over one of the orthogonal polarizations, i.e., VP/RHCP or HP/LHCP, of a dual-polarization antenna or a pair of single-polarization antennas.

Each transmitted signal is passed through the dual-polarization channel with XPI, including effects such as imperfect XPD of the antennas at the transmitter and the receiver and depolarization due to atmospheric conditions [1], [3], such as

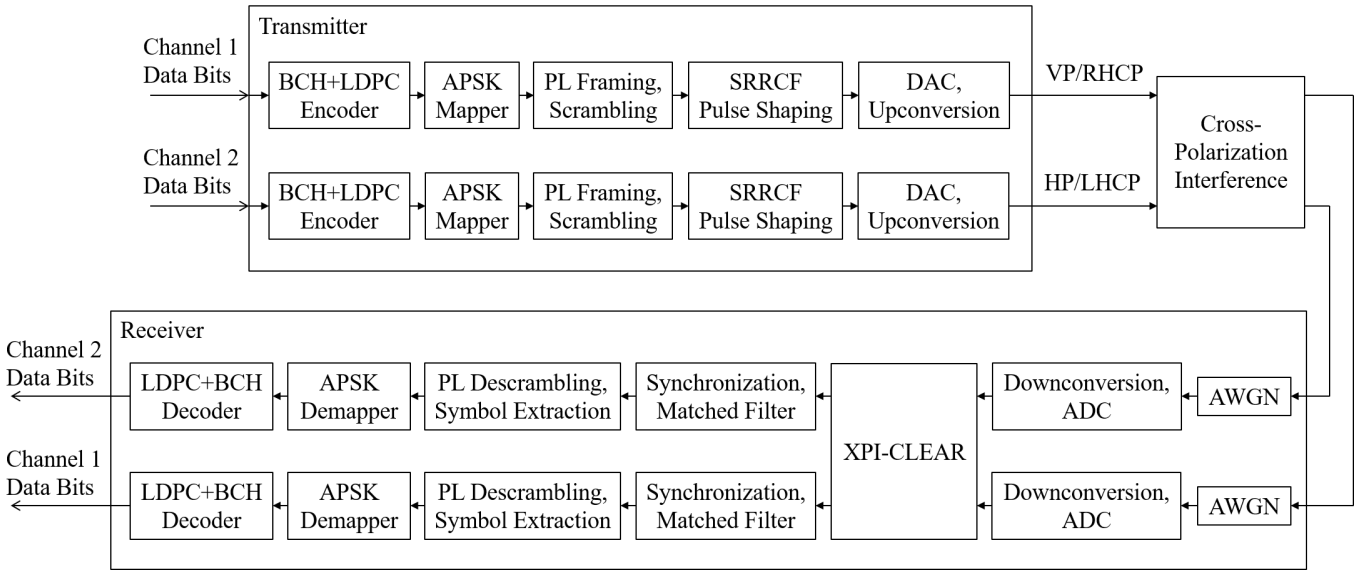

Fig. 1: Block diagram of the dual-polarization satellite transmission chain.

the hydrometeor-induced cross-polarization in the atmospheric propagation channel [12]. The XPI in satellite links for Earth observation [1], [3] is dependent on the elevation of the satellite, and a cumulative XPD of down to 17 dB can be expected for Ka-band links [1].

At the dual-channel receiver of the ground station, the signals of the two polarizations are acquired by a dual-polarization antenna or a pair of single-polarization antennas. The signals are amplified by means of a low-noise amplifier, and they are distorted by additive white Gaussian noise (AWGN). In the following receiver blocks, each signal is down-converted to baseband, and passed through an analog-to-digital converter (ADC). In this paper, an XPI compensation method, XPI-CLEAR, is employed to reduce the XPI in the two signals. In the following, after synchronization, matched filtering and downsampling, the received PL frames in each channel are produced which are then descrambled to extract the received symbols. These are then demapped, deinterleaved and decoded, to obtain the received data bits.

B. XPI Channel Modelling

The signals of the two polarizations consist of two respective streams of digital samples over time. At the receiver, the samples in each of the two streams are stored in buffers to obtain blocks of N samples, represented as row vectors, where $n = 1, \ldots, N$ is the sample index in the currently processed vector, and the buffer size N is an even number. Therefore, the current pair of output signal row vectors of the two polarizations after the XPI channel, $\mathbf{p}_1$ and $\mathbf{p}_2$, are expressed in terms of the input signal row vectors before the XPI channel, $\mathbf{x}_1$ and $\mathbf{x}_2$, as follows:

$$\mathbf{p}_1 = \sqrt{1-\gamma}\mathbf{x}_1 + \sqrt{\gamma}\exp(i\phi\pi/180)\mathbf{x}_2, \quad (1)$$

$$\mathbf{p}_2 = \sqrt{1-\gamma}\mathbf{x}_2 + \sqrt{\gamma}\exp(i\phi\pi/180)\mathbf{x}_1, \quad (2)$$

where the real-valued linear power-based factor γ is related to the cumulative XPD in the channel as $\mathrm{XPD[dB]} = 10\log_{10}\big((1-\gamma)/\gamma\big)$, ϕ is the phase angle in degrees accounting for depolarization due to rain and ice in the atmosphere [13], and i is the imaginary unit. Memory effects due to frequency selectivity of the XPD have been shown to have a minor impact in this scenario [10], and therefore, they have been excluded from the presentation in this paper.

A common channel effect in the transmission from a LEO satellite to a ground station is the Doppler frequency shift due to the high satellite velocity. For a carrier frequency in Ka band, e.g. $f_\mathrm{c} = 25$ GHz, and a LEO satellite velocity of 7800 m/s, the Doppler frequency shift amounts to 650 kHz. For a wideband satellite receiver with symbol rates up to 500 MBaud and practical oversampling factors greater or equal to 2.1, aliasing is avoided due to the sufficiently high sampling rates in accordance to the Nyquist theorem. Due to the similar transmission paths of the two signals in the dual-polarization transmission setup, the signals in the two channels are similarly affected by the Doppler frequency shift, and therefore this effect is insignificant for the XPI compensation. The Doppler frequency shift is then compensated in the subsequent synchronization block of the receiver.

However, when using two independent frequency converters with two independent voltage-controlled oscillators (VCOs) for the downconversion of the two channels, a differential frequency offset (DFO) between the two received signals can be introduced due to VCO instabilities. The DFO can be computed as the product of the carrier frequency, f_c, and the differential sensitivity of the two VCOs in the two channels, S_VCO, as follows: $f_\mathrm{DFO} = f_\mathrm{c} S_\mathrm{VCO}$. For example, a DFO of 500 kHz can be expected in a Ka-band satellite system for Earth observation using a 25 GHz carrier frequency and a typical differential sensitivity of the VCOs of 20 ppm. When using sampling rates, f_s, greater or equal to twice the sum of the symbol rate, B_s, and the DFO, the effect of the DFO can be modelled as an elementwise multiplication of the samples of one of the received signals with a rotating

complex exponential with increment of $360 f_{\mathrm{DFO}}/f_{\mathrm{s}}$ degrees per sample. As a result, the oversampling factor, η, and the sampling rate, $f_{\mathrm{s}} = \eta B_{\mathrm{s}}$, for a given symbol rate, B_{s}, can be chosen in accordance with the following inequality: $\eta B_{\mathrm{s}} \geq 2(B_{\mathrm{s}} + f_{\mathrm{DFO}})$. For a standard system without an XPI compensation block, the DFO is compensated in the synchronization block. However, as the DFO modifies the information of the XPI contained in each channel, it needs to be considered in the design of XPI compensation techniques.

III. XPI-CLEAR: A Transparent and Adaptive XPI Compensation

In this paper, a new digital XPI compensation method, XPI-CLEAR, is presented as part of a dual-channel satellite receiver which simultaneously processes the data transmitted on the two polarizations. Having local access to the signals on both channels, the XPI-CLEAR method is input by the oversampled signals of the two polarizations after the ADC stages. Equal path lengths in terms of, for example, cables or copper traces between the receiver antenna and the digital electronics in the two channels are required to avoid differential timing offset between the two signals over this portion of the transmission chain. In addition, two equal synchronous sampling clocks are assumed to drive the two ADCs, which is readily achievable due to colocation of the digital processing electronics, and sampling rates greater or equal to the Nyquist rate are required, which is a common premise in RF communication systems. In the presence of DFO between the two channels in the case when two independent frequency downconversion blocks are used, the sampling rate has to be sufficiently larger than the Nyquist rate to accommodate the DFO. The XPI-CLEAR block performs estimation and cancellation of the XPI in a transparent and adaptive fashion, concurrently using the signal samples on both channels. The processed signal samples of the two channels are output and respectively fed to the subsequent receiver stages, preserving all structural signal properties.

The oversampled signals of the two polarizations, received after the corresponding ADCs and including the AWGN, can be expressed as follows:

$$\mathbf{y}_1 = \mathbf{p}_1 + \mathbf{w}_1, \tag{3}$$

$$\mathbf{y}_2 = \mathbf{p}_2 + \mathbf{w}_2, \tag{4}$$

where the noise samples, $\mathbf{w}_1$ and $\mathbf{w}_2$, are assumed as independent and identically distributed (i.i.d.) over the sampled bandwidth of ηB_{s}. Using only the two received sample streams and the knowledge of the oversampling factor used at the two ADCs, the proposed XPI-CLEAR method employs the following complex-valued cross factor between the received signals of the two polarizations [9]:

$$\xi = \mathcal{G}\left\{ \frac{E\big[y_1[n] y_2^*[n]\big]}{\alpha\Big(E\big[y_{1,\mathrm{odd}}[k] y_{1,\mathrm{even}}^*[k]\big] + E\big[y_{2,\mathrm{odd}}[k] y_{2,\mathrm{even}}^*[k]\big]\Big)} \right\}, \tag{5}$$

where $E[\cdot]$ denotes expectation, $(\cdot)^*$ is the complex conjugation operator, the $\mathcal{G}\{\cdot\}$ operator applies the following function to the real and imaginary parts of its argument: $g(x) = \mathrm{Real}\big[(1 - \sqrt{1-4x^2})/(2x)\big]$, $k = 1, \ldots, N/2$, and α denotes the sampling correction factor which is evaluated by means of a numerical simulation of the signals. For a time-division multiplexing (TDM) transmission with SRRCF pulse shaping with roll-off factors between 5% and 35%, which is the case in the majority of satellite communication standards, the sampling correction factor, α, as a function of the oversampling factor, η, is depicted in Figure 2.

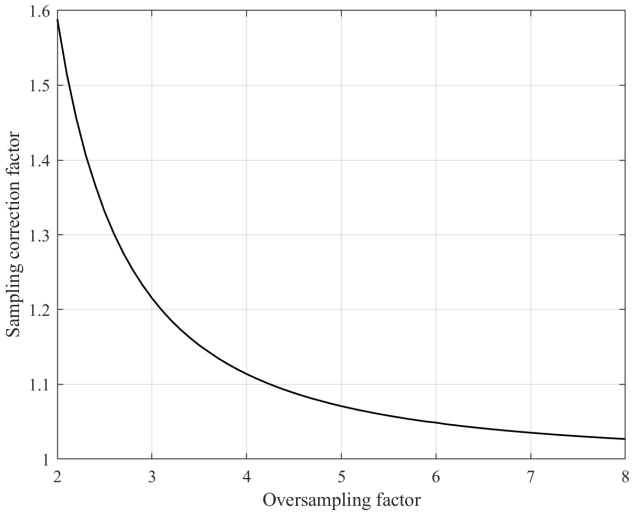

Fig. 2: Sampling correction factor as a function of the oversampling factor.

The complex-valued cross factor is used in conjunction with the two received signals, $\mathbf{y}_1$ and $\mathbf{y}_2$, to compute estimates of the XPI in the two channels as $\xi \mathbf{y}_2$ and $\xi^* \mathbf{y}_1$, respectively. The XPI cancelation is performed as the elementwise subtraction of the XPI estimates from the corresponding received signals, in order to produce the output signal samples of the XPI-CLEAR algorithm as follows [9]:

$$\mathbf{y}_{1,\mathrm{out}} = \mathbf{y}_1 - \xi \mathbf{y}_2, \tag{6}$$

$$\mathbf{y}_{2,\mathrm{out}} = \mathbf{y}_2 - \xi^* \mathbf{y}_1. \tag{7}$$

After the current pair of received signal vectors has been processed and output, the next pair of vectors of buffered received signal samples is taken, the next cross factor is computed according to (5), and it is used in the XPI cancellation in (6) and (7) to produce the next pair of output vectors of the XPI-CLEAR algorithm.

The size of the vectors $\mathbf{y}_1$ and $\mathbf{y}_2$, N, can be selected sufficiently large to provide AWGN averaging, for example, larger than 200 samples. In the case when two independent frequency converters are used for the two polarizations and there is a DFO between the two channels, the upper limit of the vector size, N, can be determined using the DFO, f_{DFO}, and the sampling rate, f_{s}, as $0.25 f_{\mathrm{s}}/f_{\mathrm{DFO}}$. As a result, the following inequality can be used as a guideline: $200 \leq N \leq 0.25 f_{\mathrm{s}}/f_{\mathrm{DFO}}$. Due to its low computational complexity, the XPI-CLEAR method is suitable for higher-

rate applications. A hardware implementation in a wideband dual-polarization satellite receiver with symbol rates up to 500 MBaud has been presented in [10].

IV. Performance Evaluation

The performance of a dual-polarization satellite receiver with the XPI-CLEAR method has been evaluated in a PDM satellite downlink transmission for Earth observation in accordance with the DVB-S2X standard [1], using two orthogonal polarizations, LHCP and RHCP, at a carrier frequency of 25 GHz in Ka band. For the data transmission in each of the two channels, a single-carrier TDM scheme with a symbol rate of 500 MBaud and a carrier roll-off of 20% in conjunction with an oversampling factor of 2, resulting in a sampling rate of 1 Gsps, is assumed. A signal waveform consisting of 100 physical layer (PL) frames is employed in each channel, where each PL frame consists of 10800 data symbols from a 16-APSK modulation format according to a $4/5$-rate LDPC code. For the operation of the XPI-CLEAR method, the vector length is set to $N = 500$. The performance is evaluated in terms of C/I and $C/(N+I)$ at the received constellation as a function of the ratio between the energy per symbol and the noise power spectral density E_s/N_0 for a variation of the parameters of the dual-polarization channel with XPI over their relevant dynamic ranges in the following scenarios:

- XPD values of 10 dB, 15 dB and 20 dB. While an XPD of 17 dB can be expected in Ka band [1], the performance of the XPI-CLEAR method is evaluated for XPD values down to 10 dB. This range also corresponds to the relevant range of switching thresholds for ACM with higher-order modulation formats.
- Phase angles of 15 degrees, 30 degrees and 45 degrees, corresponding to the range of values of the depolarization phase angle due to rain and ice in the atmosphere up to 45 degrees [1].
- DFO angle increments of 0.06 degrees, 0.12 degrees and 0.18 degrees per sample. These values correspond to DFOs of 166 kHz, 333 kHz and 500 kHz, respectively, for a carrier frequency of 25 GHz and a sampling rate of 1 Gsps.

A. Effect of the XPD

In the first scenario, the performance of the dual-polarization satellite receiver with the XPI-CLEAR method has been evaluated for XPD values of 10 dB, 15 dB and 20 dB, in order to assess the impact of variability of the XPD, e.g., due to changing elevation angles during a LEO satellite flight. For the sake of clarity, a higher XPD corresponds to a lower XPI which in turn translates to a higher C/I. The resulting C/I and $C/(N+I)$ at the received constellation as a function of the E_s/N_0 is presented in Figure 3. It should be noted that very similar performance curves resulted from tests with any modulation orders from QPSK up to 256-APSK, since the XPI-CLEAR method is transparent to the used modulation format.

The degradation of the C/I for E_s/N_0 values lower than approximately 6 dB results in only a minor degradation of the $C/(N+I)$, while the improvement of the C/I for E_s/N_0 values greater than approximately 6 dB results in a significant improvement of the $C/(N+I)$. Since the $C/(N+I)$ at the received constellation is the metric which determines the performance of the demodulator and decoder in the receiver, the degradation for $C/(N+I)$ values lower than 5 dB when using the XPI-CLEAR method is less than 1 dB for a very low XPD of 10 dB, and it is negligible for practical XPD values above 15 dB, therefore, resulting in negligible performance degradation of the receiver in this range. However, the improvements for $C/(N+I)$ values greater than 5 dB are considerable and up to 13.2 dB in the presented scenario. As a result, for lower-order modulation formats such as QPSK and 8-PSK which operate in the region of $C/(N+I)$ values lower than 5 dB, only a minor performance degradation less than 1 dB for very low XPD of 10 dB is expected, while the degradation for practical XPD values above 15 dB is negligible. For higher-order modulation formats such as 16-APSK, 32-APSK and 64-APSK which require $C/(N+I)$ values greater than 5, significant performance improvements are expected. These results justify the suitability of the XPI-CLEAR method for application with ACM.

The gains of the C/I at midrange E_s/N_0 of 14 dB are 6.9, 6.9 and 5.7 dB for, XPD values of 10, 15 and 20 dB, respectively. These increase to 16.2, 13.6 and 9.5 dB at higher E_s/N_0 of 26 dB. The gains of the $C/(N+I)$ at midrange E_s/N_0 of 14 dB are 3.7, 1.9 and 0.7 dB. These increase to 13.2, 9.4 and 5.4 dB at higher E_s/N_0 of 26 dB. The XPI-CLEAR method enables the use of the simulated $4/5$-rate 16-APSK modulation at an XPD of 10 dB, since it reaches the required $C/(N+I)$ of 11 dB, and gains of 1.8 and 0.4 dB in terms of the required E_s/N_0 are presented for practical XPD values of 15 and 20 dB, respectively. The presented considerable improvements in energy efficiency and the enabled use of higher-order modulation with practical XPD values down to as low as 10 dB show that the proposed XPI-CLEAR method is a practical solution to increase the spectral efficiency of the air interface, translating not only into increased data rates but also achieving the doubling of the throughput of the satellite link by the use of PDM.

B. Effect of the phase angle

In the second scenario, the performance of the dual-polarization satellite receiver with the XPI-CLEAR method has been evaluated for a practical XPD of 15 dB and phase angles of 15, 30 and 45 degrees, in order to assess the impact of depolarization due to atmospheric conditions. Here, a phase angle of 45 degrees represents the worst-case value [1]. The C/I and the $C/(N+I)$ at the received constellation are presented as a function of the E_s/N_0 in Figure 4. While this setup has no impact on the performance of a receiver without the XPI-CLEAR method, it shows a dependence of the performance of the XPI-CLEAR method on the phase angle of the XPI.

The gains of the C/I at midrange E_s/N_0 of 14 dB are 5.8, 3.7 and 2 dB for an XPD of 15 dB and phase angles of 15, 30 and 45 degrees, respectively. These increase to 9.4, 5.2 and

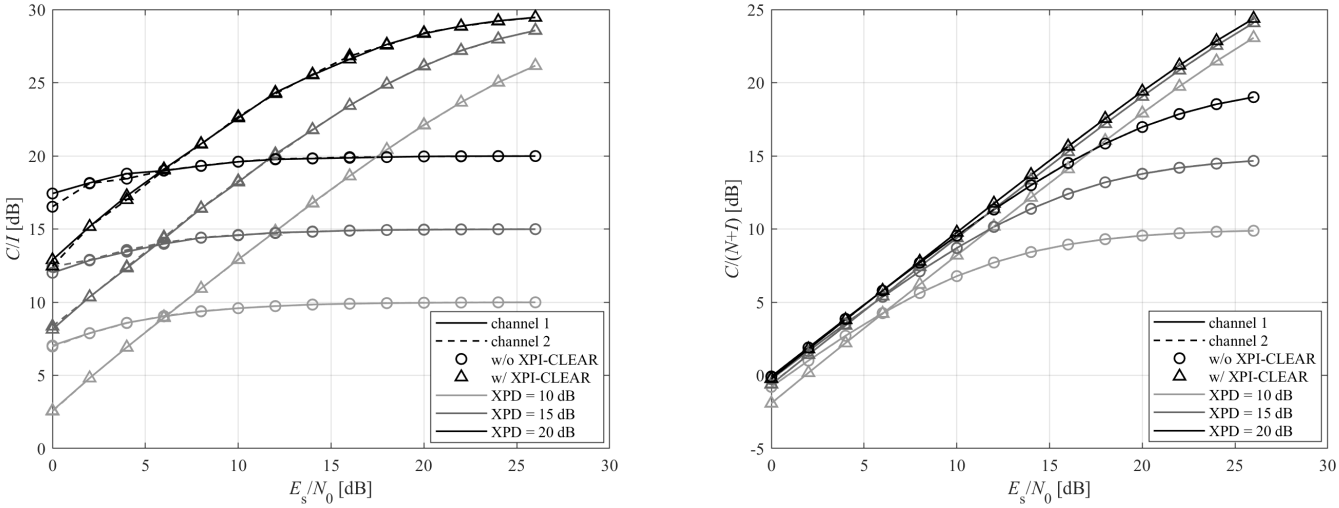

(a) C/I (b) $C/(N+I)$

Fig. 3: Comparison of the received power ratios as a function of E_s/N_0 for XPD values of 10, 15 and 20 dB.

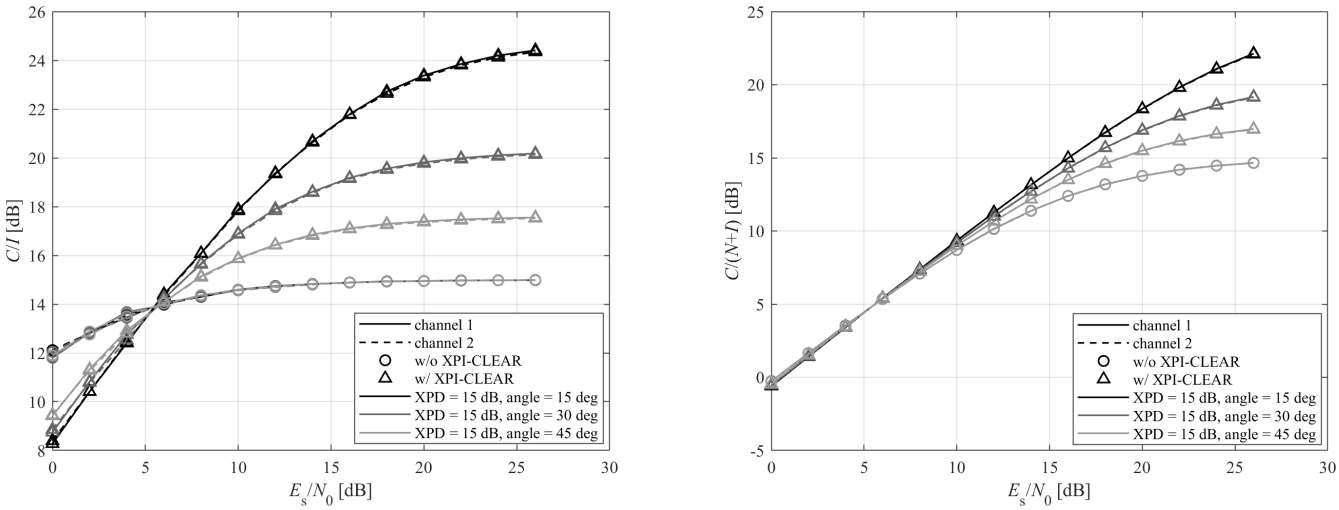

(a) C/I (b) $C/(N+I)$

Fig. 4: Comparison of the received power ratios as a function of E_s/N_0 for an XPD of 15 dB and phase angles of 15, 30 and 45 degrees.

2.5 dB at higher E_s/N_0 of 26 dB. The gains of the $C/(N+I)$ at midrange E_s/N_0 of 14 dB are 1.8, 1.3 and 0.8 dB. These increase to 7.4, 4.5 and 2.3 dB at higher E_s/N_0 of 26 dB. For the simulated $4/5$-rate 16-APSK modulation at $C/(N+I)$ of 11 dB, gains of 1.7, 1.4 and 1 dB, respectively, in terms of the required E_s/N_0 are presented with the application of the XPI-CLEAR method.

C. Effect of the DFO

In the third scenario, the performance of the dual-polarization satellite receiver with the XPI-CLEAR method has been evaluated for a practical XPD of 15 dB and a DFO with phase increments of 0.06, 0.12 and 0.18 degrees per sample, in order to assess the impact of DFO between the samples of the two channels. Here, the vector length of $N = 500$ is considered as the upper value of the inequality $200 \leq N \leq 0.25 f_\mathrm{s}/f_\mathrm{DFO}$, and so it determines the worst-case value of the phase increment of the DFO as 0.18 degrees for a differential sensitivity between the VCOs in the two channels of $S_\mathrm{VCO} = 20$ ppm and the considered setup parameters. While in a practical system an oversampling factor of 2.1 will be used to prevent aliasing, the performance of the setup in this simulation using an oversampling factor of 2 and modeling the DFO only as a multiplicative exponential with a phase

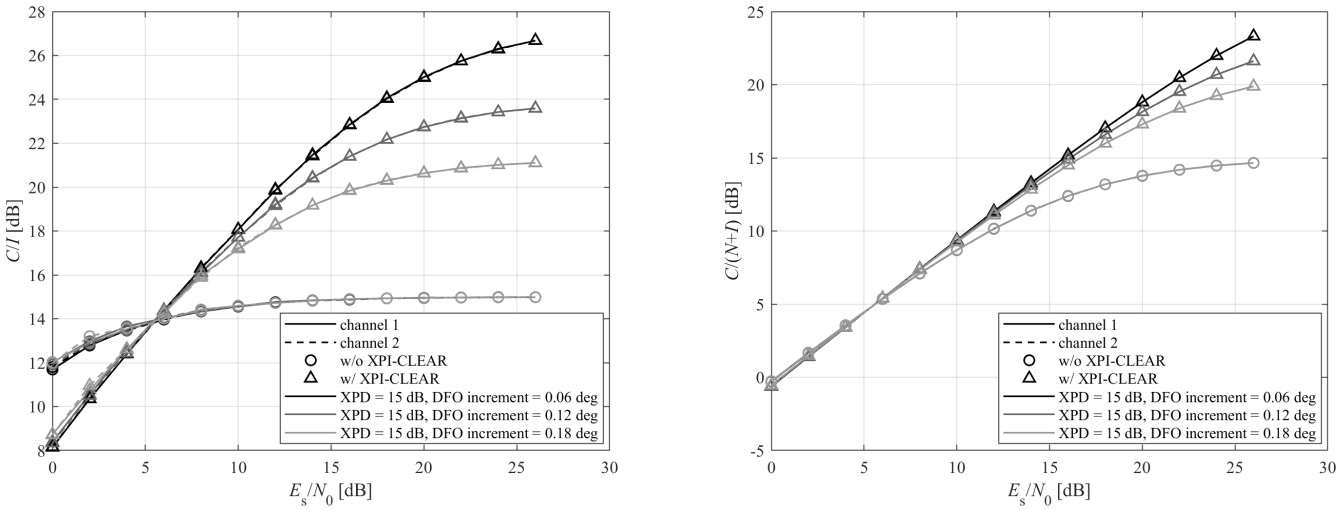

(a) C/I (b) $C/(N+I)$

Fig. 5: Comparison of the received power ratios as a function of E_s/N_0 for an XPD of 15 dB and a DFO with phase increments of 0.06, 0.12 and 0.18 degrees.

increment per sample without aliasing is considered very close to the performance of the practical system. The C/I and the $C/(N+I)$ at the received constellation are presented as a function of the E_s/N_0 in Figure 5. While this setup has no impact on the performance of a receiver without the XPI-CLEAR method, since the DFO is compensated in the synchronization block, it shows a dependence of the performance of the XPI-CLEAR method on the phase increment of the DFO.

The gains of the C/I at midrange E_s/N_0 of 14 dB are 6.6, 5.6 and 4.4 dB for an XPD of 15 dB and a DFO with phase increments of 0.06, 0.12 and 0.18 degrees per sample, respectively. These increase to 11.7, 8.6 and 6.1 dB at higher E_s/N_0 of 26 dB. The gains of the $C/(N+I)$ at midrange E_s/N_0 of 14 dB are 1.9, 1.7 and 1.5 dB. These increase to 8.7, 7 and 5.2 dB at higher E_s/N_0 of 26 dB. For the simulated $4/5$-rate 16-APSK modulation at $C/(N+I)$ of 11 dB, gains of 1.7, 1.6 and 1.5 dB, respectively, in terms of the required E_s/N_0 are presented with the application of the XPI-CLEAR method.

V. Conclusion

In this paper, a new digital blind and transparent XPI compensation method, XPI-CLEAR, has been presented for application in dual-polarization satellite receivers for wideband PDM satellite communication links. The received C/I and $C/(N+I)$ performance of the receiver with the XPI-CLEAR method has been assessed in the XPI channel with effects such as imperfect XPD of the antennas at the transmitter and the receiver, depolarization due to atmospheric conditions, and DFO between the two channels. The application of the XPI-CLEAR method has shown considerable improvements of the received $C/(N+I)$ for the studied XPI channel effects, e.g. up to 13.2 dB, proving particularly beneficial for higher-order modulation. Due to its low computational complexity, the XPI-CLEAR method is suitable for higher-rate applications. As a result, the XPI-CLEAR method is a practical solution to increase the data rates of the satellite air interface and to achieve the doubling of the throughput of the satellite link by the use of PDM, translating into higher link throughput and a lower cost per transmitted bit.

Acknowledgment

This work has been supported by the German Federal Ministry for Education and Research under contract 16KIS1247. (Das diesem Bericht zugrundeliegende Vorhaben wurde mit Mitteln des Bundesministeriums für Bildung und Forschung unter dem Förderkennzeichen 16KIS1247 gefördert.)

References

[1] "Implementation Guidelines for the Second Generation System for Broadcasting, Interactive Services, News Gathering and Other Broadband Satellite Applications; Part II: S2-Extensions (DVB-S2X), ETSI TR 102 376-2," Mar. 2015.

[2] T. Kaneko, H. Saito, M. Mita, and Y. Ohikata, "Dual Circularly Polarization X Band 2Gbps Downlink Communication System of Earth Observation Satellite," in *Proc. AIAA/USU Small Satellite Conference (AIAA/USU SSC 2018)*, Utah, USA, Aug.4-9 2018.

[3] "Flexible Advanced Coding and Modulation Scheme for High Rate Telemetry Applications, CCSDS 131.2-B-1," Mar. 2012.

[4] L. Rossi, C. Salvaneschi, M. Nava, and A. Miletic, "Interference Erasing System with Independent Receivers, EP1365519B1," Dec. 2005.

[5] J.-P. Millerioux, E. Peragin, H. Guillon, J.-L. Issler, T. Dehaene, P. Bataille, Y. Richard, G. Guillois, J. Batbedat, F. Sepot, and G. Richard, "Preliminary Definition of a High Performance X-Band Transmitter for Microsatellites," in *Proc. of The 4S Symposium 2012*, Portoroz, Slovenia, Jun.4-8 2012.

[6] M. Kawai, "Cross Polarization Interference Compensation Method, and Cross Polarization Interference Compensating Device, EP1940061A1," Jul. 2008.

[7] M. Sellathurai, P. Guinand, and J. Lodge, "Space-Time Coding in Mobile Satellite Communications Using Dual-Polarized Channels," *IEEE Trans. Veh. Technol.*, vol. 55, no. 1, pp. 188–199, Jan. 2006.

[8] P. Henarejos and A. I. Perez-Neira, "Dual Polarized Modulation and Reception for Next Generation Mobile Satellite Communications," *IEEE Trans. Commun.*, vol. 63, no. 10, pp. 3803–3812, Oct. 2015.
[9] S. Dimitrov, "Method for Receiving Two Digital Signals in a Dual-Polarization Digital Communication System, WO2023/161084A1," Aug. 2023.
[10] S. Dimitrov, V. Dantona, and G. Mocker, "Design and Implementation of Transparent Cross-Polarization Interference Compensation in a Wide-band Dual-Polarization Satellite Receiver," *Int. J. Satell. Commun. Netw.*, vol. 42, no. 6, pp. 481–492, Aug. 2024.
[11] A. Jayaprakash, B. G. Evans, P. Xiao, A. B. Awoseyila, and Y. Zhang, "New Radio Numerology and Waveform Evaluation for Satellite Integration into 5G Terrestrial Network," in *Proc. IEEE International Conference on Communications (IEEE ICC 2020)*, Dublin, Ireland, Jun.7-11 2020.
[12] "Propagation Data and Prediction Methods Required for the Design of Earth-Space Telecommunication Systems, ITU-R P.618-13," Dec. 2017.
[13] W. P. Overstreet and C. W. Bostian, "The Phase of the Crosspolarized Signal Generated By Millimeter Wave Propagation Through Rain, NASA-CR-159894," Jun. 1978.